

## Unified trade-off optimization of quantum harmonic Otto engine and refrigerator

Varinder Singh <sup>1,\*</sup>, Satnam Singh <sup>2,†</sup>, Obinna Abah<sup>3,4</sup> and Özgür E. Müstecaplıoğlu <sup>5,6</sup>

<sup>1</sup>*Center for Theoretical Physics of Complex Systems, Institute for Basic Science (IBS), Daejeon 34126, Korea*

<sup>2</sup>*Department of Physical Sciences, Indian Institute of Science Education and Research Mohali, Sector 81, S.A.S. Nagar, Manauli PO 140306, Punjab, India*

<sup>3</sup>*Centre for Theoretical Atomic, Molecular and Optical Physics, School of Mathematics and Physics, Queen's University Belfast, Belfast BT7 1NN, United Kingdom*

<sup>4</sup>*School of Mathematics, Statistics, and Physics, Newcastle University, Newcastle upon Tyne NE1 7RU, United Kingdom*

<sup>5</sup>*Department of Physics, Koç University, 34450 Sarıyer, Istanbul, Turkey*

<sup>6</sup>*TÜBİTAK Research Institute for Fundamental Sciences, 41470 Gebze, Turkey*



(Received 2 January 2022; accepted 9 August 2022; published 31 August 2022)

We investigate quantum Otto engine and refrigeration cycles of a time-dependent harmonic oscillator operating under the conditions of maximum  $\Omega$  function, a trade-off objective function which represents a compromise between energy benefits and losses for a specific job, for both adiabatic and nonadiabatic (sudden) frequency modulations. We derive analytical expressions for the efficiency and coefficient of performance of the Otto cycle. For the case of adiabatic driving, we point out that in the low-temperature regime, the harmonic Otto engine (refrigerator) can be mapped to Feynman's ratchet and pawl model which is a steady-state classical heat engine. For the sudden switch of frequencies, we obtain loop-like behavior of the efficiency-work curve, which is characteristic of irreversible heat engines. Finally, we discuss the behavior of cooling power at maximum  $\Omega$  function.

DOI: [10.1103/PhysRevE.106.024137](https://doi.org/10.1103/PhysRevE.106.024137)

### I. INTRODUCTION

Since the dawn of the industrial revolution, thermal machines have provided the practical impetus to the development of thermodynamics on the experimental and theoretical front. The discovery of Carnot efficiency, which sets a universal upper bound on the efficiency of all heat engines working between two reservoirs, led to the formulation of the second law of thermodynamics by Clausius [1]. Heat engines and refrigerators are the two well-known examples of thermal devices. Heat engines convert thermal energy into useful mechanical work while the refrigerators use external work to lower the temperature of the target system [2]. These machines require at least two heat reservoirs at different temperatures, and their performance is limited by the Carnot bound. In the case of heat engines, the Carnot efficiency is given by,  $\eta_C = 1 - \beta_2/\beta_1$ , where  $\beta_i = 1/(k_B T_i)$ , ( $i = 1, 2$ ) is the inverse temperature of the two reservoirs ( $\beta_1 > \beta_2$ ) and  $k_B$  is the Boltzmann constant [2,3]. The corresponding bound on the coefficient of performance (COP) of the refrigerators is given by,  $\zeta_C = \beta_2/(\beta_1 - \beta_2)$ . Moreover, the last six decades have witnessed a great interest in understanding the interplay between thermodynamics and quantum mechanics. In recent time, experimental realization of quantum machines has been demonstrated [4,5]; for a review, see Ref. [6].

However, practical performance of the heat engines and refrigerators are usually lower than the optimal per-

formance due to the associated heat leaks and frictional effects [7–10]. The goal of finite-time thermodynamics is finding the optimal performance of thermal machines when these limitations are taken into account as well as devising ways to improve on it [11–14]. One is usually interested in optimizing the power output of a heat engine and its corresponding efficiency [15–26], whereas, for a refrigerator, the most desirable figure of merit is cooling power [14,27–29]. A well-known observation is that the thermal engines operating at maximum power also dissipate a large amount of power due to entropy production, which ultimately pollutes the environment [10,30–32]. Therefore, instead of operating engines (refrigerators) in the maximum power (cooling power) regime, the real irreversible thermal machines should operate near the maximum power point where they yield considerably higher efficiency with a significant reduction in entropy production. The ecological function [33],  $\Omega$  function [34], and efficient power function [35,36] are the most commonly studied trade-off objective functions which pay equal attention to both efficiency and power.

Furthermore, the rapid development in the field of quantum technologies has bring up the question of resource consumption in the thermodynamic landscape (see Ref. [37]). Thus, quantum thermodynamic devices offer the natural avenue to address the fundamental limits of energy consumption at the quantum level. Therefore, while optimizing quantum thermal devices, one should choose an objective function which pays equal attention to both efficiency and power of the engine, thereby taking care of the environmental and energetic considerations.

\* varinder@ibs.re.kr

† satnamphysics@gmail.com

However, due to its simplicity and amenability to analytical results, a quantum Otto cycle, whose working substance is a time-dependent single harmonic oscillator, has become a standard model to investigate the performance characteristics of thermal devices [22,38–50]. Furthermore, the recent experimental realization of a nanoscale harmonic Otto heat engine provides us with better motivation to study its thermodynamic performance in great detail [5]. Although there have been some studies [40,41,51] investigating the optimal performance of harmonic Otto heat engines and refrigerators, many aspects remained to be explored, such as performance analysis in the low-temperature regime where both the reservoirs are at low temperatures. Furthermore, an analytic expression for the COP of the refrigerator is still missing in the sudden limit of operation.

This paper explores the optimization of  $\Omega$  function for the Otto cycle, whose working substance is a quantum harmonic oscillator. In particular, the  $\Omega$  function allows a unified trade-off between useful energy delivered and energy lost for heat engines and refrigerators [34,44], which makes it an ideal figure of merit to study optimal performance of both engines and refrigerators on equal footing. We carry out an extensive analysis of the two extreme limiting cases of operation of the Otto cycle: adiabatic limit, which corresponds to quasistatic expansion and compression strokes, and sudden limit of expansion and compression strokes. In both cases, we obtain analytic results for the efficiency (COP) at maximum  $\Omega$  function of the heat engine (refrigerator).

The rest of the paper is organized as follows: In Sec. II we discuss the model of a harmonic Otto cycle coupled to two thermal reservoirs at different temperatures. Section III presents analytic expressions for the efficiency at maximum  $\Omega$  function for both adiabatic and nonadiabatic frequency driving in high- and low-temperature limits. Furthermore, we show the loop-like behavior of efficiency-work curve of the engine operation. In Sec. IV, we present the analysis of the quantum Otto cycle when it is functioning as a refrigerator in both adiabatic as well as nonadiabatic frequency modulations in different temperature regimes. We present the conclusions in Sec. V.

## II. QUANTUM OTTO CYCLE

The quantum Otto cycle consists two adiabatic and two isochoric thermodynamic processes. These four steps occur in the following order [41,51]: (1) Adiabatic compression  $A \rightarrow B$ : Initially, we assume the system is thermalized at inverse temperature  $\beta_1$ . Then, the system is isolated from the environment and the frequency of the oscillator is changed from  $\omega_1$  to  $\omega_2$  via an external driving protocol. The average energy of the system increases the work being done on the system. The evolution is unitary, and the von Neumann entropy of the system remains constant. (2) Hot isochore  $B \rightarrow C$ : During this stage, the harmonic oscillator is in contact with the hot bath at inverse temperature  $\beta_2$ , and frequency ( $\omega_2$ ) of the oscillator is kept fixed at a fixed value. The system exchanges energy with the hot bath and attains the same temperature of the hot reservoir. In this work, we are assuming that the working fluid is fully thermalized in the finite time. In general, the evolution of the system in contact with the heat reservoirs

is modeled by the Lindblad master equation. For the quantum harmonic Otto cycle, all details are presented in Ref. [40]. Our case can be considered as a special case of general time evolution given by Lindblad master equation when heat conductivity coefficients become very large, hence allowing for thermalization in finite-time. (3) Isentropic expansion  $C \rightarrow D$ : The system is isolated from the surroundings, and the frequency of the harmonic oscillator is unitarily brought back to its initial value  $\omega_1$ . Work is done by the system in this stage. (4) Cold isochore  $D \rightarrow A$ : To bring back the working fluid (harmonic oscillator) to its initial state, the system is placed in contact with the cold reservoir at inverse temperature  $\beta_1$  ( $\beta_1 < \beta_2$ ) at fixed frequency  $\omega_1$ , and is allowed to relax back to the initial thermal state  $A$ .

The average energies  $\langle H \rangle$  of the oscillator at the four stages of the cycle are ( $\hbar = 1$ ) [41,51]

$$\langle H \rangle_A = \frac{\omega_1}{2} \coth\left(\frac{\beta_1 \omega_1}{2}\right), \quad (1)$$

$$\langle H \rangle_B = \frac{\omega_2}{2} \lambda \coth\left(\frac{\beta_1 \omega_1}{2}\right), \quad (2)$$

$$\langle H \rangle_C = \frac{\omega_2}{2} \coth\left(\frac{\beta_2 \omega_2}{2}\right), \quad (3)$$

$$\langle H \rangle_D = \frac{\omega_1}{2} \lambda \coth\left(\frac{\beta_2 \omega_2}{2}\right), \quad (4)$$

where  $\lambda$  is the dimensionless adiabaticity parameter of the dynamics which depends on the nature of the frequency modulation, see Refs. [52,53] for details. In general, we have  $\lambda \geq 1$ , and the general form of  $\lambda$  is given by

$$\lambda = \frac{1}{2\omega_1\omega_2} \left\{ \omega_1^2 [\omega_2^2 X(t)^2 + \dot{X}(t)^2] + [\omega_2^2 Y(t)^2 + \dot{Y}(t)^2] \right\},$$

where  $X(t)$  and  $Y(t)$  are the solutions of the equation  $d^2X/dt^2 + \omega^2(t)X = 0$  satisfying  $X(0) = 0$ ,  $\dot{X}(0) = 1$ ,  $Y(0) = 1$ ,  $\dot{Y}(0) = 0$  [52,53]. The expressions for mean heat exchanged during the hot and cold isochores can be evaluated, respectively, as follows:

$$Q_2 = \langle H \rangle_C - \langle H \rangle_B = \frac{\omega_2}{2} \left[ \coth\left(\frac{\beta_2 \omega_2}{2}\right) - \lambda \coth\left(\frac{\beta_1 \omega_1}{2}\right) \right], \quad (5)$$

$$Q_4 = \langle H \rangle_A - \langle H \rangle_D = \frac{\omega_1}{2} \left[ \coth\left(\frac{\beta_1 \omega_1}{2}\right) - \lambda \coth\left(\frac{\beta_2 \omega_2}{2}\right) \right]. \quad (6)$$

We are employing a sign convention in which all the incoming fluxes (heat and work) are taken to be positive.

## III. QUANTUM OTTO HEAT ENGINE

Here, we consider when the quantum Otto cycle whose working medium is a time-dependent modulated harmonic oscillator is functioning as a heat engine. Since the working fluid returns to its initial state after one complete cycle, the net work done on the system in a cycle is given by the first law of thermodynamics,  $W = -(Q_2 + Q_4)$ . Work is said to be extracted from the engine when  $W_{\text{ext}} = -W = Q_2 + Q_4 > 0$ .

Accordingly, the efficiency of the engine is given by [17]

$$\eta = \frac{W_{\text{ext}}}{Q_2} = 1 - \frac{\omega_1 \coth(\beta_1 \omega_1/2) - \lambda \coth(\beta_2 \omega_2/2)}{\omega_2 \lambda \coth(\beta_1 \omega_1/2) - \coth(\beta_2 \omega_2/2)}. \quad (7)$$

The optimal performance of the harmonic Otto engine at maximum work or power has been studied already [41]. In this work, we optimize the  $\Omega$  function, which represents a compromise between the useful work and the loss of work in the system [34]. It is defined as [34]

$$\Omega = 2W_{\text{ext}} - \eta_{\text{max}} Q_2, \quad (8)$$

where  $\eta_{\text{max}} \leq \eta_C$  is the maximum possible efficiency achievable to the engine under consideration. The  $\Omega$  function is equivalent to another trade-off function known as ecological function when  $\eta_{\text{max}} = \eta_C$  [33,34]. For the harmonic Otto cycle,  $\eta_{\text{max}}$  depends on the speed of the adiabatic protocol which is expressed in terms  $\lambda$  [42]. We will show in a moment that, in the adiabatic case,  $\eta_{\text{max}} = \eta_C$ . However, in the case of nonadiabatic work strokes, the maximum efficiency of the engine under consideration is always less than the Carnot efficiency due to internal friction. Particularly, for the sudden-switch case, the maximum efficiency of the engine is given by Eq. (27) [42]. In the following, we first discuss the adiabatic case and then move on to discuss nonadiabatic scenario.

### A. Adiabatic case

Quantum adiabatic processes are much slower than the typical timescales of the system. In this case, the adiabaticity parameter  $\lambda$  is equal to unity, i.e.,  $\lambda = 1$ . To make things more transparent, we want to add that evolution at zero rate is not necessary to avoid entropy production. This can be achieved by various means, such as using shortcuts to adiabaticity techniques [54] or suppressing coherence terms by employing quantum lubrication [55]. However, such control schemes have their own cost to maintain the adiabaticity of the system [56]. In this work, we focus on simple and analytical tractable two extremals of quantum Otto machines performance.

From the positive work condition,  $W_{\text{ext}} = Q_2 + Q_4 > 0$ , we find  $\eta_{\text{max}} = \eta_C$ . Using Eqs. (7) and (8), the expressions for efficiency and  $\Omega$  function take the forms

$$\eta = 1 - \frac{\omega_1}{\omega_2}, \quad \Omega = 2W_{\text{ext}} - \eta_C Q_2. \quad (9)$$

### 1. High-temperature regime

To obtain analytic expression in closed form for the efficiency at maximum  $\Omega$  function, we will first study the high-temperature regime. In the high-temperature regime, we set  $\coth(\beta_i \omega_i/2) \approx 2/(\beta_i \omega_i)$  ( $i = 1, 2$ ). Using Eqs. (5) and (6) in Eq. (9), the expression for  $\Omega$  function is written as

$$\Omega = \frac{(z - \tau)(1 + \tau - 2z)}{\beta_2 z}, \quad (10)$$

where  $z \equiv \omega_1/\omega_2$  is the compression ratio of the Otto cycle, and  $\tau = \beta_2/\beta_1$ . Optimization of Eq. (10) with respect to compression ratio  $z$  yields  $z^* = \sqrt{\tau(1 + \tau)}/2$ . Hence, the efficiency at maximum  $\Omega$  function, in terms of Carnot efficiency,

is given by

$$\eta_{\text{high}}^{\Omega} = 1 - \sqrt{\frac{(1 - \eta_C)(2 - \eta_C)}{2}}, \quad (11)$$

which concurs with the efficiency of the endoreversible and symmetric low-dissipation models of heat engines [33,57]. The results are not surprising as in the high-temperature regime (classical regime), the engines are expected to behave like classical heat engines [27,31,58]. Equation (11) was first obtained by Angulo-Brown for the optimization of endoreversible heat engines [33]. The corresponding efficiency for the optimization of the harmonic Otto engine operating under the conditions of maximum work output is given by Curzon-Ahlborn formula,  $\eta_{\text{high}}^W = \eta_{\text{CA}} = 1 - \sqrt{1 - \eta_C}$  [40,41]. See Eqs. (18) and (22) for the comparison of  $\eta_{\text{high}}^W$  and  $\eta_{\text{high}}^{\Omega}$ . It is clear that  $\eta_{\text{high}}^{\Omega}$  is always greater than  $\eta_{\text{high}}^W$ , which is expected outcome [33,34].

### 2. Low-temperature regime

Here, we discuss the performance of the harmonic Otto engine in the low-temperature regime which has not been explored in earlier publications. In Refs. [41,51,59], the optimization has been carried out in the regime defined by the constraints  $\beta_1 \omega_1 \gg 1$  and  $\beta_2 \omega_2 \ll 1$ , i.e., the hot reservoir being very hot and the cold reservoir being very cold. In the following, we discuss adiabatic case only as it is not possible to obtain analytic results for the nonadiabatic case. We assume that  $\beta_i \omega_i \gg 1$ , and set  $\coth(\beta_i \omega_i/2) \approx 1 + 2e^{-\beta_i \omega_i}$ . Using Eqs. (5) and (6) in the expression,  $W_{\text{ext}} = Q_2 + Q_4$ , the extracted work, in the low-temperature limit, can be expressed as follows:

$$W_{\text{ext}}^{\text{low}} = (\omega_2 - \omega_1)(e^{-\beta_2 \omega_2} - e^{-\beta_1 \omega_1}). \quad (12)$$

Apart from a multiplicative constant, the above expression for extracted work is similar to the expression for the power output of the Feynman's ratchet and pawl model, where control parameters are internal energy states  $\epsilon_1$  and  $\epsilon_2$  instead of  $\omega_1$  and  $\omega_2$  [60–63]. Thus in the low-temperature limit, the harmonic Otto engine can be mapped to Feynman's model, which is a steady-state classical heat engine based on the principle of Brownian fluctuations [60,61]. Interestingly, it is not the only case in which a quantum heat engine can be mapped to Feynman's ratchet and pawl engine. Recently, a three-level laser quantum heat engine operating in the low-temperature regime was also mapped to Feynman's model [31].

To make the physics of the connection of the quantum Otto cycle with the Feynman ratchet more transparent, we note that, in the low-temperature regime, only first two levels of the working fluid will be occupied. Initially, when system is in equilibrium with the cold reservoir at inverse temperature  $\beta_1$ , the probability of finding the system in the upper (lower) level can be approximated by  $e^{-\beta_1 \omega_1}$  ( $1 - e^{-\beta_1 \omega_1}$ ) [39]. During the adiabatic compression stroke  $B \rightarrow C$  (see Fig. 1) when frequency of the harmonic oscillator is varied from  $\omega_1$  to  $\omega_2$ , the occupation probabilities of the levels do not change. During the hot isochore, the working fluid absorbs heat from the reservoir and the occupation probability of the upper (lower) level increases (decreases). The net change in the occupation probability of the upper (lower) level is given

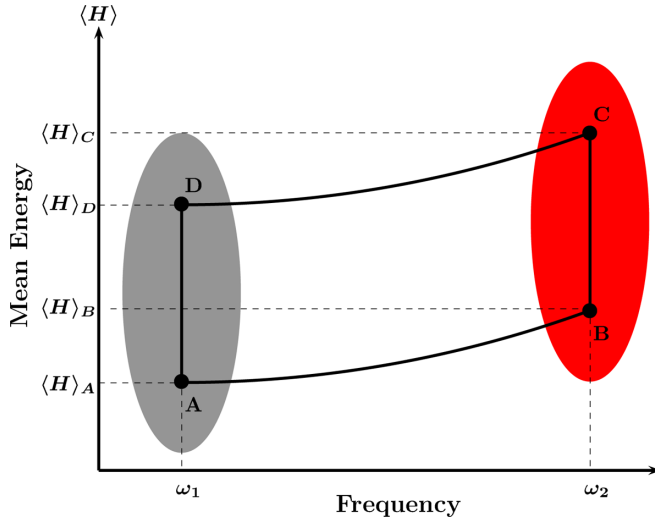


FIG. 1. Pictorial depiction of Otto cycle. The thermodynamic cycle consists of four stages: two adiabatic (A  $\rightarrow$  B and C  $\rightarrow$  D) and two isochoric (B  $\rightarrow$  C and D  $\rightarrow$  A) steps.

by  $\Delta p_{\text{upper}} = e^{-\beta_2 \omega_2} - e^{-\beta_1 \omega_1}$  ( $\Delta p_{\text{lower}} = -\Delta p_{\text{upper}}$ ), which is exactly equal to the net jump frequency of the Feynman's ratchet and pawl system. Since the Hamiltonian of the system does not change during the isochoric steps, multiplication of  $\Delta p_{\text{upper}}$  with the energy gap  $\omega_2$  (recall,  $\hbar = 1$ ) yields the heat absorbed from the hot reservoir, which has the same form as that of Feynman's ratchet and pawl system. Similar argument also holds for the heat rejected to the cold reservoir at constant frequency  $\omega_1$ .

Additionally, we can look at Eq. (12) from a fundamental point of view of the general processes described by its terms. The frequency  $\omega_2$  associated with the hot isochore (cf. Fig. 1) can be envisioned as the energy required for compressing the spring in the ratchet-pawl system. This energy cost comes from the hot reservoir at a rate given by the first term in the second factor in Eq. (12). As a result, the pawl makes a forward (jumps up) motion at a rate  $R_F = e^{-\beta_2 \omega_2}$ . In contrast, the second term is the rate for backward (jumps down) motion of the pawl,  $R_B = e^{-\beta_1 \omega_1}$ . A finite, nonzero displacement is associated with the ordered energy provided by a torque  $L$  multiplied by an angular displacement  $\Delta\theta$  in the case of the ratchet-pawl system. In our case, the difference in the working system (oscillator) excitation energies plays a role as the work done by the torque in the ratchet-pawl system, i.e.,  $\omega_2 - \omega_1$ , is equivalent to  $L\Delta\theta$ . Accordingly, in a time interval of  $\Delta t$ , the work done for a ratchet-pawl system can be written as  $W = (L\Delta\theta)(R_F - R_B)\Delta t$  [54] or for harmonic-oscillator Otto cycle, equivalently as in Eq. (12). Heat intake from the hot bath can also be expressed similarly. Due to the generic form of work and heat equations, the efficiency at maximum power calculation of the harmonic oscillator yields the same results as the ratchet-pawl system, first derived in Ref. [60], which is highly nonlinear due to the exponential rates. This nonlinearity is reflected in the efficiency expressions [cf. Eqs. (15) and (17)] and Eq. (12). Nonlinearity plays a fundamental role in the nature of irreversibility of the ratchet system [64–66], and hence for the quantum harmonic-oscillator Otto cycle.

In the linear ratchet regime [67], the efficiency of maximum power expression reduces to that of exoreversible [64,68,69] finite-time thermodynamics systems, where only internal dissipation can exist while there is no heat dissipated to the cold bath.

To obtain the analytic expression for the efficiency which is independent of the parameters of the system and depends on the ratio of bath temperatures only, the optimization should be carried out with respect to two variables ( $\omega_1$  and  $\omega_2$ ) simultaneously. Treating  $\omega_1$  and  $\omega_2$  as the independent variables, optimization of Eq. (12) with respect to  $\omega_1$  and  $\omega_2$  yields the following optimal solution:

$$\omega_1^* = \frac{(1 - \eta_C)[\eta_C - \ln(1 - \eta_C)]}{\eta_C \beta_2}, \quad (13)$$

$$\omega_2^* = \frac{\eta_C - (1 - \eta_C) \ln(1 - \eta_C)}{\eta_C \beta_2}. \quad (14)$$

Using Eqs. (13) and (14) in Eqs. (9) and (12), we obtain the expressions for the efficiency at maximum  $\Omega$  function and optimal work, respectively;

$$\eta_{\text{low}}^W = \frac{\eta_C^2}{\eta_C - (1 - \eta_C) \ln(1 - \eta_C)}, \quad (15)$$

$$W_{\text{ext}}^{\text{low}*} = \frac{\eta_C^2 (1 - \eta_C)^{(1 - \eta_C)/\eta_C}}{\beta_2 e}. \quad (16)$$

Using these analytic expressions, we discuss the universal nature of efficiency at maximum work. For near-equilibrium conditions, expanding ( $\beta_1 \approx \beta_2$ ) Eq. (15) in Taylor series, we have

$$\eta_{\text{low}}^W = \frac{\eta_C}{2} + \frac{\eta_C^2}{8} + \frac{7\eta_C^3}{96} + O(\eta_C^4). \quad (17)$$

For comparison, we also present the Taylor series expansion of  $\eta_{\text{high}}^W$ ,

$$\eta_{\text{high}}^W = \frac{\eta_C}{2} + \frac{\eta_C^2}{8} + \frac{6\eta_C^3}{96} + O(\eta_C^4). \quad (18)$$

Notice that  $\eta_{\text{low}}^W > \eta_{\text{high}}^W$ . The first two terms in both Eqs. (17) and (18) are  $\eta_C/2$  and  $\eta_C^2/8$ , and third term is model dependent. For heat engines obeying tight-coupling condition (no heat leaks), universality of first term  $\eta_C/2$  was proven by Van den Broeck using the formalism of linear irreversible thermodynamics [70]. Furthermore, the universality of second term can be proved by invoking the symmetry of Onsager coefficients on the nonlinear level [24].

Similarly, for the optimization of the  $\Omega$  function, the optimal solution is given by [31]

$$\omega_1^\Omega = \frac{[\eta_C + (2 - \eta_C)k]}{\beta_1 \eta_C}, \quad \omega_2^\Omega = \frac{[\eta_C + 2k(1 - \eta_C)]}{\beta_1 \eta_C (1 - \eta_C)}, \quad (19)$$

where  $k = \ln[(2 - \eta_C)/2(1 - \eta_C)]$ . We obtain the efficiency at maximum  $\Omega$  function and its optimal  $\Omega$  function as follows:

$$\eta_{\text{low}}^\Omega = \frac{\eta_C + (1 - \eta_C)k}{\eta_C + 2(1 - \eta_C)k} \eta_C, \quad (20)$$

$$\Omega_{\text{low}}^* = \frac{\eta_C^2 [2(1 - \eta_C)]^{2(1 - \eta_C)/\eta_C}}{\beta_2 e (2 - \eta_C)^{(2 - \eta_C)/\eta_C}}. \quad (21)$$

Similar to the case of work optimization,  $\eta_{\text{low}}^{\Omega}$  is independent of the parameters of the system (harmonic oscillator) and depends on ratio of reservoir temperatures ( $\beta_2/\beta_1$ ) only. Now, we turn to the universal nature of efficiency. The universal nature of efficiency is not unique feature of the optimization of work or power output of the engine, the efficiency at maximum  $\Omega$  function also shows universal behavior [71]. Taking near-equilibrium series expansions of Eqs. (11) and (20), we have

$$\eta_{\text{high}}^{\Omega} = \frac{3\eta_C}{4} + \frac{\eta_C^2}{32} + \frac{18\eta_C^3}{768} + O(\eta_C^4), \quad (22)$$

$$\eta_{\text{low}}^{\Omega} = \frac{3\eta_C}{4} + \frac{\eta_C^2}{32} + \frac{19\eta_C^3}{768} + O(\eta_C^4). \quad (23)$$

Again, it is self evident from Eqs. (22) and (23) that first two terms of  $\eta_{\text{high}}^{\Omega}$  and  $\eta_{\text{low}}^{\Omega}$  are same, and the model dependent differences appear in the third term only. The universality of the efficiency at maximum  $\Omega$  function was first formally proven by Zhang and coauthors [71] by using the framework of stochastic thermodynamics. The first two terms  $3\eta_C/4$  and  $\eta_C^2/32$  were also obtained for endoreversible [33,72], low-dissipation [57], minimally nonlinear irreversible [73] and some other models of classical and quantum heat engines [31,72,74].

### B. Sudden switch of frequencies

Next, we discuss the case in which frequency of the oscillator is changed suddenly from one value to the other. In this case,  $\lambda = (\omega_1^2 + \omega_2^2)/2\omega_1\omega_2$  [52]. The efficiency is no longer given by Eq. (9), and expression for the efficiency, in the high-temperature limit, reads

$$\eta_{\text{SS}} = \frac{(z^2 - 1)(z^2 - \tau)}{\tau + (\tau - 2)z^2}, \quad (24)$$

where  $z \equiv \omega_1/\omega_2$  is the compression ratio of the Otto cycle, and  $\tau = \beta_2/\beta_1$ . Similarly, the expression for the extracted work is given by

$$W_{\text{ext}}^{\text{SS}} = \frac{(1 - z^2)(z^2 - \tau)}{2z^2\beta_2}. \quad (25)$$

From the positive work condition  $W_{\text{SS}} > 0$  we have

$$z^2 > \tau \Rightarrow z > \sqrt{\tau}. \quad (26)$$

The above condition is more restrictive than the positive work condition for the adiabatic case which implies that  $z > \tau$ . Hence, for the given temperatures of the cold and hot reservoirs, it is more difficult to extract work for the sudden-switch case as compared with the adiabatic one.

Here, we are interested in the optimization of the  $\Omega$  function. To find the expression for the  $\Omega$  function, first we have to specify  $\eta_{\text{max}}$ . Recently, the form of  $\eta_{\text{max}}$  is evaluated in Ref. [42] and reads

$$\eta_{\text{max}}^{\text{SS}} = \frac{[3 - \eta_C - 2\sqrt{2(1 - \eta_C)}]\eta_C}{(1 + \eta_C)^2} \leq \frac{1}{2}. \quad (27)$$

Substituting Eq. (27) into Eq. (9), we obtain required expression for the  $\Omega$  function for the nonadiabatic (sudden-switch)

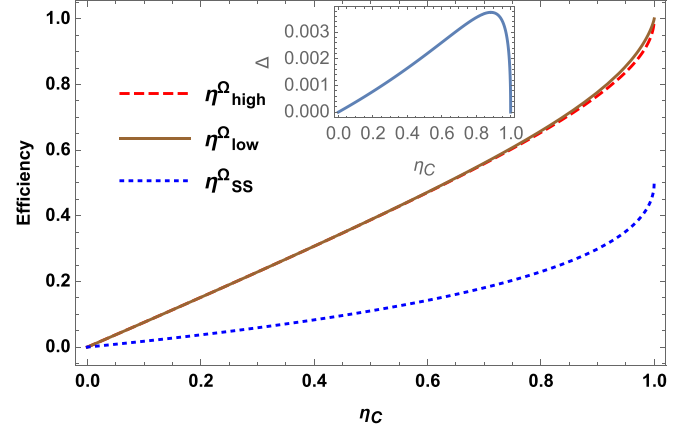


FIG. 2. Efficiency at maximum  $\Omega$  function as a function of Carnot efficiency. For adiabatic case; the red dashed curve represents the high-temperature limit, Eq. (11), while the solid brown curve correspond to the low-temperature regime, Eq. (20). The blue dotted curve corresponds to the sudden-switch case at the high-temperature, Eq. (29). The inset shows the difference ( $\Delta$ ) between the efficiency at maximum  $\Omega$  function,  $\eta_{\text{SS}}^{\Omega}$  [Eq. (29)], and efficiency at maximum work,  $\eta_{\text{SS}}^W = (1 - \sqrt{1 - \eta_C})/(2 + \sqrt{1 - \eta_C})$ , as a function of Carnot efficiency.

case as follows:

$$\Omega_{\text{SS}} = \frac{(1 - z^2) \left( 2(z^2 - \tau) + \frac{(\tau - 1)(\tau - 2\sqrt{2}\sqrt{\tau + 2})[\tau + (\tau - 2)z^2]}{(\tau - 2)^2(z^2 - 1)} \right)}{2z^2}. \quad (28)$$

Then by optimizing the  $\Omega$  function, the efficiency at maximum  $\Omega$  function is obtained as

$$\eta_{\text{SS}}^{\Omega} = \frac{(2 + 2\eta_C - A)(2 - 2\eta_C^2 - A)}{2(1 + \eta_C)^2(2 - 2\eta_C - A)}, \quad (29)$$

where  $A = \{2(1 - \eta_C)[2 + \eta_C + 2\eta_C\sqrt{2(1 - \eta_C)} + 3\eta_C^2]\}^{1/2}$ . This efficiency can be considered as the counterpart of the efficiency at maximum work,  $\eta_{\text{SS}}^W = (1 - \sqrt{1 - \eta_C})/(2 + \sqrt{1 - \eta_C})$ , which was obtained for the optimization of the work output of the quantum harmonic Otto engine undergoing sudden compression and expansion strokes during the adiabatic branches [40].

To compare the performance of the engine for the adiabatic driving and sudden-switch case, we plot Eqs. (11) and (20) along with the expression for Eq. (29) in Fig. 2 as a function of Carnot efficiency. In the inset of Fig. 2, we have plotted the difference between  $\eta_{\text{SS}}^W$  and  $\eta_{\text{SS}}^{\Omega}$ . Although in the sudden-switch case, the efficiency at maximum  $\Omega$  function is larger than the efficiency at maximum work, the difference is not substantial. Furthermore, the efficiency at maximum  $\Omega$  function is very low in the sudden-switch regime as compared with the adiabatic driving. We attribute this to the highly frictional nature of the sudden-switch regime as explained below. In the sudden-switch case, the sudden change of the frequency of the harmonic oscillator induces nonadiabatic transitions between its energy levels and leaves the system in a highly nonequilibrium state. In terms of the energy eigenstates of the instantaneous Hamiltonian, the off-diagonal terms of the density matrix, known as coherences, are nonzero. Generating coherences give rise to extra energetic cost when compared

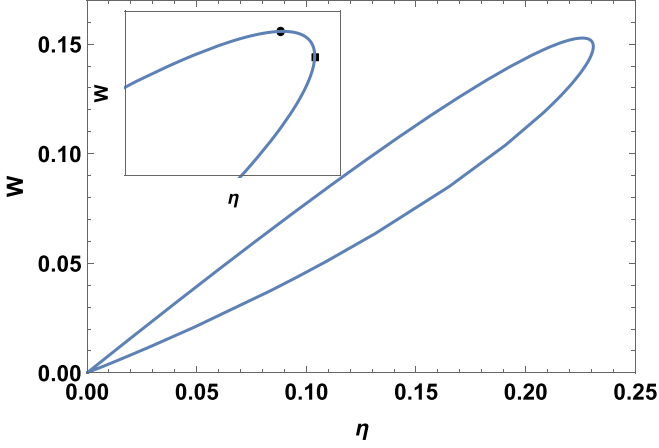


FIG. 3. Loop shaped work versus efficiency curve, characteristic of real irreversible heat engines. The parametric plot is generated using Eqs. (24) and (25) for the fixed value of  $\tau = 0.2$ . In the inset, we have plotted the amplified version of efficiency-work curve to distinguish the maximum work and maximum efficiency points. Maximum efficiency (black dot) and maximum work (square dot) points lie very close to each other.

with adiabatic driving, and an additional parasitic internal energy is stored in the working medium. This extra cost gets dissipated to the heat reservoirs during the preceding isochoric stages of the cycle and is termed as quantum friction [20,55,75–78]. Therefore, the inner friction is detrimental for the performance of the engine under consideration.

Now, we present the typical efficiency-work curves in Fig. 3. Using Eqs. (24) and (25), the parametric plot between work and efficiency is obtained (see, Fig. 3). The efficiency-work ( $\eta, W$ ) curve shows the loop-like behavior, characteristic of realistic irreversible heat engines [8,9,79,80]. As shown in Fig. 3, the maximum efficiency and maximum work output points lie extremely close to each other. The optimal operating regime of the nonadiabatic engine under consideration is situated on the part of ( $\eta, W$ ) curve, which has a negative slope; that is, the portion of the ( $\eta, W$ ) curve lying in between maximum work and maximum efficiency point. The optimization of the  $\Omega$  function lies in this regime. It is worth mentioning that the loop shape of the work efficiency curve arises due to the presence of inner friction in the operation of the engine which is a purely quantum-mechanical effect, as mentioned earlier. The loop-like behavior can also be seen in power-efficiency curve of classical endoreversible heat engines in the presence of heat leaks in the system [10,81].

However, the loop-shape ( $\eta, W$ ) curves are not exclusive to the sudden switch strokes heat engine considered here. They can be obtained for any adiabatic stroke happening in finite time, thus giving rise to nonadiabatic transitions between the energy levels of the harmonic oscillator, which are responsible for the appearance of inner friction. As time spent on adiabatic branches increases, the maximum work and maximum efficiency points on the ( $\eta, W$ ) curve will move further apart. Finally, for the quasistatic process, the ( $\eta, W$ ) curve will become open parabolic in shape, just like the efficiency-power curve of endoreversible heat engines without heat leaks [8–10].

#### IV. QUANTUM OTTO REFRIGERATOR

In this section, we investigate the performance of the harmonic Otto cycle working as a refrigerator in the adiabatic as well as nonadiabatic regime. For the refrigerator,  $Q_4 > 0$ ,  $Q_2 < 0$ , and the work invested to transport heat from the cold reservoir to the hot reservoir is positive,  $W_{\text{in}} = -(Q_2 + Q_4) > 0$ . The coefficient of performance (COP) of the refrigerator is defined as

$$\zeta = \frac{Q_4}{W_{\text{in}}} = -\frac{Q_4}{Q_2 + Q_4}. \quad (30)$$

Using Eqs. (5) and (6) in Eq. (30), the COP takes the following form [51]:

$$\zeta = \frac{\omega_1 [\coth(\beta_1 \omega_1 / 2) - \lambda \coth(\beta_1 \omega_1 / 2)]}{(\lambda \omega_2 - \omega_1) \coth(\frac{\beta_1 \omega_1}{2}) - (\omega_2 - \lambda \omega_1) \coth(\frac{\beta_2 \omega_2}{2})}. \quad (31)$$

The  $\Omega$  function for the refrigerator is given by [34]

$$\Omega = 2Q_4 - \zeta_{\text{max}} W_{\text{in}}, \quad (32)$$

where  $\zeta_{\text{max}} \leq \zeta_C$  is the maximum COP with which our refrigerator can operate. From Eq. (32), the  $\Omega$  function is different for adiabatic and nonadiabatic driving refrigerator. Similar to the heat engine, when  $\zeta_{\text{max}} = \zeta_C$ , the  $\Omega$  function is equivalent to the ecological function [82] defined for refrigerators. We first discuss the adiabatic case and then proceed to the sudden-switch case.

##### A. Adiabatic driving

Let now consider the adiabatic case,  $\lambda = 1$ , the COP in Eq. (31) takes the following form,

$$\zeta_{\text{ad}} = \frac{\omega_1}{\omega_2 - \omega_1} = \frac{z}{1 - z}, \quad (33)$$

where  $z = \omega_1 / \omega_2$  is the compression ratio of the Otto cycle. Similarly, substituting  $\lambda = 1$  in Eq. (6), the positive cooling condition,  $Q_4 > 0$ , implies that  $\beta_1 \omega_1 < \beta_2 \omega_2$ , which in turn implies that  $\zeta < \zeta_C$ . Hence, for the adiabatic driving,  $\zeta_{\text{max}} = \zeta_C$ . Therefore, from Eq. (32), we have

$$\Omega = 2Q_4 - \zeta_C W_{\text{in}}. \quad (34)$$

##### 1. High-temperature regime

Again, to evaluate analytic expressions for the COP, we choose to work in the high-temperature regime. In this regime, using Eqs. (5), (6) along with  $W_{\text{in}} = -(Q_2 + Q_4)$ ,  $\Omega$  function can be written in terms of temperature ratio ( $\tau$ ) and  $z$  as,

$$\Omega = \frac{(z - \tau)[\tau - z(2 - \tau)]}{\beta_2 z(1 - \tau)}. \quad (35)$$

Optimization of  $\Omega$  function with respect to  $z$  yields the following optimal solution,

$$z^* = \frac{\tau}{\sqrt{2 - \tau}}. \quad (36)$$

Substituting Eq. (36) into Eq. (33), we have

$$\zeta_{\text{high}}^{\Omega} = \frac{\tau}{\sqrt{2 - \tau} - \tau} = \frac{\zeta_C}{\sqrt{(1 + \zeta_C)(2 + \zeta_C)} - \zeta_C}. \quad (37)$$

Equation (37), the COP of harmonic Otto refrigerator operating at high-temperature and adiabatic regime. It is the same as those of the endoreversible [82] and symmetric low-dissipation models of heat engines [57]. The corresponding COP at maximum  $\chi$ -criterion, which is the product of the COP and cooling power ( $Q_4$ ) of a refrigerator, is given by the formula,  $\zeta_{\text{high}}^{\chi} = \sqrt{1 + \zeta_C} - 1$  [51]. Our numerical analysis (not presented here) show that  $\zeta_{\text{high}}^{\chi}$  is always lower than  $\zeta_{\text{high}}^{\Omega}$ .

## 2. Low-temperature regime

In the low-temperature case, the expressions for  $Q_4$  and  $\Omega$  take the forms:

$$Q_4 = \omega_1(e^{-\beta_1\omega_1} - e^{-\beta_2\omega_2}), \quad (38)$$

$$\Omega = [(2 + \zeta_C)\omega_1 - \zeta_C\omega_2](e^{-\beta_1\omega_1} - e^{-\beta_2\omega_2}). \quad (39)$$

Performing the two-parameter optimization of Eq. (39) with respect to control parameters  $\omega_1$  and  $\omega_2$ , the optimal solution is obtained as [83]

$$\omega_1^* = \frac{1 - (1 + \zeta_C)k}{\beta_1}, \quad \omega_2^* = \frac{1 - (2 + \zeta_C)k}{\beta_2}, \quad (40)$$

where  $k = \ln[(1 + \zeta_C)/(2 + \zeta_C)]$ . Substituting above expressions for  $\omega_1$  and  $\omega_2$  into Eq. (33), the expression for the optimal COP reads

$$\zeta_{\text{low}}^{\Omega} = \frac{1 - (1 + \zeta_C)k}{1 - 2(1 + \zeta_C)k} \zeta_C. \quad (41)$$

Similar to the case of heat engine, COP of the refrigerator does not depend on the system parameters and depends on the ratio of the reservoir temperatures  $\tau$  only. As we have shown that the adiabatic harmonic Otto cycle operating in the low-temperature regime can be mapped to Feynman's model, the above expression also holds for the optimization of Feynman's ratchet and pawl model [84] and a three-level laser quantum refrigerator [83]. For comparison, Eq. (37) (solid yellow curve) and Eq. (41) (dotted red curve) are plotted in Fig. 4. It can be seen that they are practically indistinguishable for the entire range of the graph. This can be understood by looking at the Taylor series behavior of  $\zeta_{\text{high}}^{\Omega}$  and  $\zeta_{\text{low}}^{\Omega}$  near equilibrium:

$$\zeta_{\text{high}}^{\Omega} = \frac{2\zeta_C}{3} + \frac{1}{18} - \frac{17}{216\zeta_C} + O\left(\frac{1}{\zeta_C^3}\right), \quad (42)$$

$$\zeta_{\text{low}}^{\Omega} = \frac{2\zeta_C}{3} + \frac{1}{18} - \frac{16}{216\zeta_C} + O\left(\frac{1}{\zeta_C^3}\right). \quad (43)$$

The first two terms of on the right-hand side of the above equations are the same and the third term is negligible for any value of  $\zeta_C > 1$ , thus explaining the overlap of curves representing  $\zeta_{\text{high}}^{\Omega}$  and  $\zeta_{\text{low}}^{\Omega}$  in Fig. 4.

## B. Sudden switch of frequencies

Next, we discuss the case in which frequency of the oscillator is changed suddenly from the initial frequency to the final frequency. In this case,  $\lambda = (\omega_1^2 + \omega_2^2)/2\omega_1\omega_2$ . The optimal performance of the harmonic Otto refrigerator operating in the sudden-switch regime has not been fully explored earlier. In Ref. [51], the performance of the refrigerator was studied for

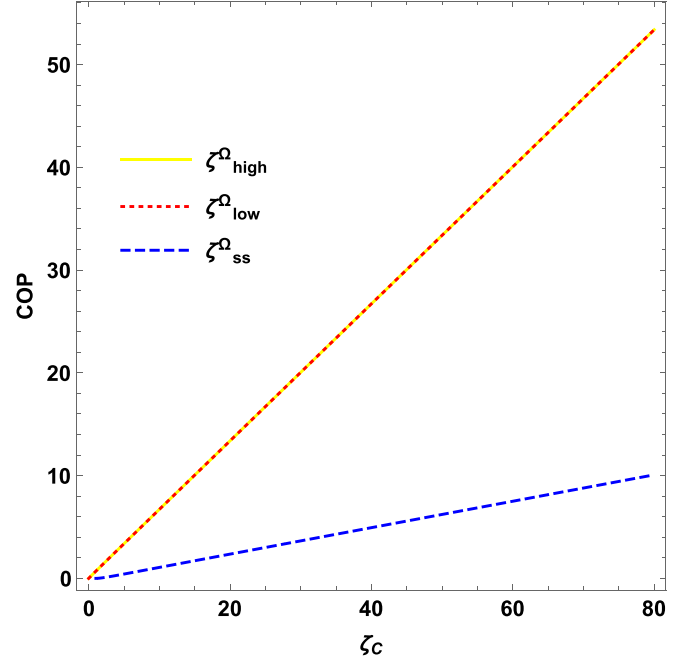


FIG. 4. Coefficient of performance (COP) at the maximum  $\Omega$  function versus Carnot COP. The yellow solid line represents the COP at maximum  $\Omega$  function in the high-temperature regime [Eq. (37)] while the red dotted line corresponds to the COP at maximum  $\Omega$  function in the low-temperature regime [Eq. (41)]. The blue dashed line corresponds to the case of sudden switch at high-temperature [Eq. (49)].

weak nonadiabatic driving (for adiabaticity parameter  $\lambda$  close to 1), and the analytic expression for corresponding minimal driving time was obtained. In the sudden-switch regime, the cooling power does not exhibit a generic maximum with respect to control parameter  $z$ , i.e., the maximum of the cooling power is obtained for  $z = 0$ , which is clearly not a useful result. Hence, to study the optimal operation of the refrigerator working under the conditions of maximum  $\Omega$  function is a sensible option. Here, we obtain the analytic expression for the COP at optimal  $\Omega$  function.

For a sudden-switch driving protocol, the expression for the cooling power and input work are

$$Q_4 = \frac{1}{\beta_2} \left[ \tau - \frac{1}{2}(z^2 + 1) \right], \quad W_{\text{total}} = \frac{(z^2 - 1)(z^2 - \tau)}{2\beta_2 z^2}. \quad (44)$$

Furthermore, the COP  $\zeta_C = Q_4/W_{\text{in}}$  takes the form

$$\zeta_{\text{ss}} = \frac{z^2(2\tau - z^2 - 1)}{(z^2 - 1)(z^2 - \tau)}. \quad (45)$$

To proceed, we have to specify form of maximum COP. Recently, in Ref. [42], using the positive cooling condition, it was shown that in the sudden-switch regime, the maximum COP of the harmonic Otto refrigerator is no longer given by Carnot COP  $\zeta_C$ . The desired form of maximum COP, which is much tighter than the Carnot bound, is found to be [42]

$$\zeta_{\text{max}} = 1 + 3\zeta_C - 2\sqrt{2\zeta_C(1 + \zeta_C)}. \quad (46)$$

Another interesting constraint imposed by the condition  $Q_4 > 0$  on the temperatures of the reservoirs is

$$\tau > 1/2 \text{ or } \zeta_C > 1. \quad (47)$$

The above condition has interesting implications on the performance of the Otto refrigerator operating in the sudden-switch regime. Equation (47) simply implies that the thermal machine under consideration cannot work as a refrigerator unless the temperature of the cold reservoir is greater than  $T_2/2$ .

Using Eqs. (44) and (46) in Eq. (32), the desired form of  $\Omega$  function can be evaluated and optimized to yield the following optimal solution

$$z^* = \frac{\zeta_C[1 + 3\zeta_C - 2\sqrt{2\zeta_C(1 + \zeta_C)}]}{(1 + \zeta_C)[3(1 + \zeta_C) - 2\sqrt{2\zeta_C(1 + \zeta_C)}]}. \quad (48)$$

Substituting Eq. (48) into Eq. (45), we find the expression for the COP at maximum  $\Omega$  function as follows:

$$\zeta_{ss}^\Omega = \frac{A[1 - \zeta_C + A(1 + \zeta_C)]}{(A - 1)[\zeta_C - A(1 + \zeta_C)]}, \quad (49)$$

where  $A = \{\zeta_C[1 + 3\zeta_C - 2\sqrt{2\zeta_C(1 + \zeta_C)}]/(1 + \zeta_C)[3(1 + \zeta_C) - 2\sqrt{2\zeta_C(1 + \zeta_C)}]\}^{1/2}$ . We have plotted Eq. (49) as a function of  $\zeta_C$  in Fig. 4 (dashed blue curve). As expected, COP for the sudden-switch case is much smaller than the corresponding COPs obtained for the adiabatic case.

### C. Cooling power at maximum $\Omega$ function

In all the cases discussed above, cooling power is maximum at  $z = 0$ , which is not a useful result. To look more into the behavior of cooling power, here, we will discuss the behavior of the cooling power at maximum  $\Omega$  function. First, for the case of the adiabatic driving in the high-temperature limit, substituting the optimal solution  $z^* = \tau/\sqrt{2 - \tau}$  [see Eq. (36)] into  $Q_4 = (\tau - z)/\beta_2$  yields the following expression for the cooling power:

$$Q_{4(ad)}^{\Omega(\text{high})} = \frac{1}{\beta_2} \left( \tau - \frac{\tau}{\sqrt{2 - \tau}} \right). \quad (50)$$

Similarly, for the adiabatic driving in the low-temperature regime, substituting Eq. (40) into Eq. (38), we obtain

$$Q_{4(ad)}^{\Omega(\text{low})} = \frac{\left(\frac{1}{2-\tau}\right)^{\frac{1}{1-\tau}} [1 - \tau - \ln\left(\frac{1}{2-\tau}\right)] \tau}{e\beta_2(2 - \tau)}. \quad (51)$$

where  $e$  is Euler's number,  $e = 2.718$ . Finally, from Eqs. (48) and (44), the cooling power at maximum  $\Omega$  function for the sudden-switch case is given by

$$Q_{4(ss)}^\Omega = \frac{1}{2\beta_2} \left( 2\tau - \sqrt{\frac{\tau(2\tau - 2\sqrt{2\tau} + 1)}{3 - 2\sqrt{2\tau}}} - 1 \right). \quad (52)$$

We plot cooling power [i.e., Eqs. (50)–(52)] as a function of  $\tau$  for a fixed value of  $\beta_2$  in Fig. 5. It is clear from the figure that the maximum of cooling power exists at some value of  $\tau$  for each case discussed. We observe that despite the

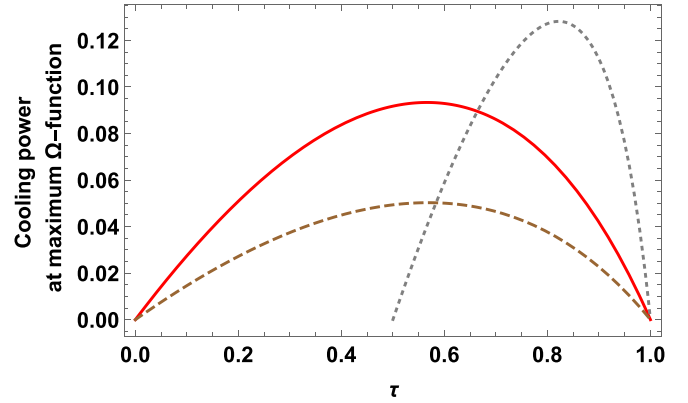


FIG. 5. Cooling power at maximum  $\Omega$  function against ratio of reservoir temperatures ( $\tau$ ) for a fixed value of  $\beta_2 = 1$ . For the adiabatic case, the red solid curve corresponds to the cooling power in the high-temperature regime [Eq. (50)] while the brown dashed curve is the cooling in the low-temperature regime [Eq. (51)]. The gray dotted curve represents the cooling power for the sudden-switch scenario in the high-temperature regime [Eq. (52)].

sudden-switch operation offering the highest possible cooling power, the possible range of its operation is limited. Thus, this provides a guide of the best choice for optimal operation of a harmonic Otto refrigerator depending on the available resources. We remark that this kind of behavior is not exclusive to the harmonic Otto refrigerator as it was recently observed for a three-level quantum refrigerator [83].

## V. CONCLUSIONS

We have investigated the optimal performance of a harmonic quantum Otto cycle working under the conditions of maximum  $\Omega$  function. First, we obtained the analytic expressions for the efficiency at maximum  $\Omega$  function of the engine in the adiabatic driving regime for both high- and low-temperature regimes. In particular, for the heat engine operation in the low-temperature regime, we showed that the harmonic Otto engine can be mapped to a classical heat engine known as Feynman's ratchet and pawl model. Then, in the nonadiabatic driving regime in which we suddenly modulate the frequency of the oscillator from its initial to final value, we obtained loop-shaped curves for the efficiency-work plot characterizing the irreversible behavior of the engine under consideration. We repeated our analysis to study the optimal performance of the Otto refrigerator and obtained corresponding analytic expressions for the coefficient of performance (COP) of the refrigerator. Furthermore, we explored the behavior of the cooling power under the conditions of maximum  $\Omega$  function.

## ACKNOWLEDGMENTS

This research was supported by the Institute for Basic Science in Korea (IBS-R024-Y2 and IBS-R024-D1). O.A. acknowledges support from the UK EPSRC EP/S02994X/1.

- [1] D. Kondepudi and I. Prigogine, *Modern Thermodynamics: From Heat Engines to Dissipative Structures* (Wiley, New York, 1998).
- [2] Y. Cengel and M. Boles, *Thermodynamics. An Engineering Approach* (McGraw-Hill, New York, 2001).
- [3] H. Callen, *Thermodynamics and an Introduction to Thermostatistics* (Wiley, New York, 1985).
- [4] J. Roßnagel, S. Dawkins, K. Tolazzi, O. Abah, E. Lutz, F. Schmidt-Kaler, and K. Singer, *Science* **352**, 325 (2016).
- [5] J. Klaers, S. Faelt, A. Imamoglu, and E. Togan, *Phys. Rev. X* **7**, 031044 (2017).
- [6] N. M. Myers, O. Abah, and S. Deffner, *AVS Quantum Sci.* **4**, 027101 (2022).
- [7] A. R. Insinga, *Entropy* **22**, 1060 (2020).
- [8] J. M. Gordon, *Am. J. Phys.* **59**, 551 (1991).
- [9] J. M. Gordon and M. Huleihil, *J. Appl. Phys.* **72**, 829 (1992).
- [10] J. Chen, Z. Yan, G. Lin, and B. Andresen, *Energy Convers. Manage.* **42**, 173 (2001).
- [11] B. Andresen, *Angew. Chem., Int. Ed.* **50**, 2690 (2011).
- [12] B. Andresen, P. Salamon, and R. S. Berry, *Phys. Today* **37**, 62 (1984).
- [13] P. Salamon, J. Nulton, G. Siragusa, T. Andersen, and A. Limon, *Energy (Oxford, U. K.)* **26**, 307 (2001).
- [14] R. Kosloff and A. Levy, *Annu. Rev. Phys. Chem.* **65**, 365 (2014).
- [15] F. L. Curzon and B. Ahlborn, *Am. J. Phys.* **43**, 22 (1975).
- [16] P. Landsberg and H. Leff, *J. Phys. A: Math. Gen.* **22**, 4019 (1989).
- [17] J. Roßnagel, O. Abah, F. Schmidt-Kaler, K. Singer, and E. Lutz, *Phys. Rev. Lett.* **112**, 030602 (2014).
- [18] S. Singh, *Int. J. Theor. Phys.* **59**, 2889 (2020).
- [19] S. Singh and S. Rebari, *Eur. Phys. J. B* **93**, 150 (2020).
- [20] R. Kosloff and Y. Rezek, *Entropy* **19**, 136 (2017).
- [21] S. Singh and O. Abah, [arXiv:2008.05002](https://arxiv.org/abs/2008.05002).
- [22] N. M. Myers and S. Deffner, *Phys. Rev. E* **101**, 012110 (2020).
- [23] N. Piccione, G. De Chiara, and B. Bellomo, *Phys. Rev. A* **103**, 032211 (2021).
- [24] M. Esposito, K. Lindenberg, and C. Van den Broeck, *Phys. Rev. Lett.* **102**, 130602 (2009).
- [25] M. Esposito, R. Kawai, K. Lindenberg, and C. Van den Broeck, *Phys. Rev. Lett.* **105**, 150603 (2010).
- [26] V. Singh, *Phys. Rev. Research* **2**, 043187 (2020).
- [27] V. Singh, T. Pandit, and R. S. Johal, *Phys. Rev. E* **101**, 062121 (2020).
- [28] L. A. Correa, J. P. Palao, G. Adesso, and D. Alonso, *Phys. Rev. E* **90**, 062124 (2014).
- [29] Y. Apertet, H. Ouerdane, A. Michot, C. Goupil, and P. Lecoeur, *Europhys. Lett.* **103**, 40001 (2013).
- [30] V. Singh and R. S. Johal, *Phys. Rev. E* **98**, 062132 (2018).
- [31] V. Singh and R. S. Johal, *Phys. Rev. E* **100**, 012138 (2019).
- [32] A. de Vos, *Endoreversible Thermodynamics of Solar Energy Conversion* (Oxford University Press, Oxford, 1992).
- [33] F. Angulo-Brown, *J. Appl. Phys.* **69**, 7465 (1991).
- [34] A. C. Hernández, A. Medina, J. M. M. Roco, J. A. White, and S. Velasco, *Phys. Rev. E* **63**, 037102 (2001).
- [35] J. W. Stucki, *Eur. J. Biochem.* **109**, 269 (1980).
- [36] T. Yilmaz, *J. Energy Inst.* **79**, 38 (2006).
- [37] A. Auffèves, *PRX Quantum* **3**, 020101 (2022).
- [38] H. T. Quan, Y.-x. Liu, C. P. Sun, and F. Nori, *Phys. Rev. E* **76**, 031105 (2007).
- [39] T. D. Kieu, *Phys. Rev. Lett.* **93**, 140403 (2004).
- [40] Y. Rezek and R. Kosloff, *New J. Phys.* **8**, 83 (2006).
- [41] O. Abah, J. Roßnagel, G. Jacob, S. Deffner, F. Schmidt-Kaler, K. Singer, and E. Lutz, *Phys. Rev. Lett.* **109**, 203006 (2012).
- [42] V. Singh and O. E. Müstecaplıoğlu, *Phys. Rev. E* **102**, 062123 (2020).
- [43] S. Saryal and B. K. Agarwalla, *Phys. Rev. E* **103**, L060103 (2021).
- [44] N. Sánchez-Salas and A. C. Hernández, *Phys. Rev. E* **70**, 046134 (2004).
- [45] B. Çakmak, *Turk. J. Phys.* **45**, 59 (2021).
- [46] V. Shaghaghi, G. M. Palma, and G. Benenti, *Phys. Rev. E* **105**, 034101 (2022).
- [47] R. J. de Assis, T. M. de Mendonça, C. J. Villas-Boas, A. M. de Souza, R. S. Sarthour, I. S. Oliveira, and N. G. de Almeida, *Phys. Rev. Lett.* **122**, 240602 (2019).
- [48] R. J. de Assis, J. S. Sales, J. A. R. da Cunha, and N. G. de Almeida, *Phys. Rev. E* **102**, 052131 (2020).
- [49] T. Pandit, P. Chattopadhyay, and G. Paul, *Mod. Phys. Lett. A* **36**, 2150174 (2021).
- [50] R. Shastri and B. P. Venkatesh, [arXiv:2204.04782](https://arxiv.org/abs/2204.04782).
- [51] O. Abah and E. Lutz, *Europhys. Lett.* **113**, 60002 (2016).
- [52] S. Deffner and E. Lutz, *Phys. Rev. E* **77**, 021128 (2008).
- [53] K. Husimi, *Prog. Theor. Phys.* **9**, 238 (1953).
- [54] D. Guéry-Odelin, A. Ruschhaupt, A. Kiely, E. Torrontegui, S. Martínez-Garaot, and J. G. Muga, *Rev. Mod. Phys.* **91**, 045001 (2019).
- [55] T. Feldmann and R. Kosloff, *Phys. Rev. E* **73**, 025107(R) (2006).
- [56] E. Torrontegui, I. Lizuain, S. González-Resines, A. Tobalina, A. Ruschhaupt, R. Kosloff, and J. G. Muga, *Phys. Rev. A* **96**, 022133 (2017).
- [57] C. de Tomás, J. M. M. Roco, A. C. Hernández, Y. Wang, and Z. C. Tu, *Phys. Rev. E* **87**, 012105 (2013).
- [58] E. Geva and R. Kosloff, *J. Chem. Phys.* **97**, 4398 (1992).
- [59] O. Abah and E. Lutz, *Europhys. Lett.* **106**, 20001 (2014).
- [60] Z. C. Tu, *J. Phys. A: Math. Theor.* **41**, 312003 (2008).
- [61] R. P. Feynman, R. B. Leighton, and M. Sands, *The Feynman Lectures on Physics* (Narosa Publishing House, New Delhi, 2008).
- [62] V. Singh and R. S. Johal, *J. Stat. Mech.: Theory Exp.* (2018) 073205.
- [63] V. Singh and R. S. Johal, *J. Stat. Mech.: Theory Exp.* (2019) 093208.
- [64] Y. Apertet, H. Ouerdane, C. Goupil, and P. Lecoeur, *Phys. Rev. E* **90**, 012113 (2014).
- [65] Y. Apertet, H. Ouerdane, C. Goupil, and P. Lecoeur, *Phys. Rev. E* **96**, 022119 (2017).
- [66] H. Ouerdane, Y. Apertet, C. Goupil, and P. Lecoeur, *Eur. Phys. J. Spec. Top.* **224**, 839 (2015).
- [67] S. Velasco, J. M. M. Roco, A. Medina, and A. C. Hernández, *J. Phys. D: Appl. Phys.* **34**, 1000 (2001).
- [68] C. W. L. Chen and F. Sun, *Appl. Therm. Eng.* **17**, 103 (1997).
- [69] T. Schmiedl and U. Seifert, *Europhys. Lett.* **81**, 20003 (2008).
- [70] C. Van den Broeck, *Phys. Rev. Lett.* **95**, 190602 (2005).
- [71] Y. Zhang, C. Huang, G. Lin, and J. Chen, *Phys. Rev. E* **93**, 032152 (2016).
- [72] N. Sánchez-Salas, L. López-Palacios, S. Velasco, and A. Calvo Hernández, *Phys. Rev. E* **82**, 051101 (2010).

- [73] R. Long, Z. Liu, and W. Liu, *Phys. Rev. E* **89**, 062119 (2014).
- [74] R. Long and W. Liu, *Phys. Rev. E* **91**, 042127 (2015).
- [75] Y. Rezek, *Entropy* **12**, 1885 (2010).
- [76] F. Plastina, A. Alecce, T. J. G. Apollaro, G. Falcone, G. Francica, F. Galve, N. Lo Gullo, and R. Zambrini, *Phys. Rev. Lett.* **113**, 260601 (2014).
- [77] T. Feldmann and R. Kosloff, *Phys. Rev. E* **61**, 4774 (2000).
- [78] S. Çakmak, F. Altintas, A. Gençten, and Ö. E. Müstecaplıoğlu, *Eur. Phys. J. D* **71**, 75 (2017).
- [79] J. P. Palao, R. Kosloff, and J. M. Gordon, *Phys. Rev. E* **64**, 056130 (2001).
- [80] G. Benenti, G. Casati, K. Saito, and R. S. Whitney, *Phys. Rep.* **694**, 1 (2017).
- [81] J. Chen, *J. Phys. D: Appl. Phys.* **27**, 1144 (1994).
- [82] Z. Yan and L. Chen, *J. Phys. D: Appl. Phys.* **29**, 3017 (1996).
- [83] K. Kaur, V. Singh, J. Ghai, S. Jena, and Ö. E. Müstecaplıoğlu, *Phys. A (Amsterdam, Neth.)* **576**, 125892 (2021).
- [84] V. Singh and R. S. Johal, *Entropy* **19**, 576 (2017).